Supporting information

# Hierarchically Compartmentalized Supramolecular Gels through Multilevel Self-Sorting

Yiming Wang,[†] Matija Lovrak,[†] Qian Liu,[†] Chandan Maity,[†] Vincent A. A. le Sage,[†] Xuhong Guo,[‡,§] Rienk Eelkema,[†] Jan H. van Esch*,[†]

[†] Department of Chemical Engineering, Delft University of Technology, van der Maasweg 9, 2629 HZ Delft, The Netherlands.

[‡] State Key Laboratory of Chemical Engineering, School of Chemical Engineering, East China University of Science and Technology, Shanghai 200237, China

[§] Engineering Research Center of Materials Chemical Engineering of Xinjiang Bingtuan, Shihezi University, Xinjiang 832000, China

*Corresponding email: j.h.vanesch@tudelft.nl

## Table of content

## Materials

Molecule **H**, **A**, **A**$^{-}$, and **A-FL** were synthesized as reported.[1-3] All commercial chemicals were purchased from Sigma Aldrich.

## Experimental and supporting discussion

### CLSM measurement

CLSM measurements were performed on a Zeiss LSM 710 confocal laser scanning microscope equipped with a Zeiss Axio Observer inverted microscope and 40x PlanFluor oil immersion objective lens (NA 1.3). Incident laser with a wavelength of 488 nm and 405 nm was used to excite the fluorescein probe and **Hoechst 33342**, respectively. The pinhole was set to 1.0 airy unit during the measurements and the data were processed using ZEN 2009 software. Fluorescence recovery after photobleaching (FRAP) experiments were performed with a 405 nm laser. Each sample was prepared in well-sealed imaging chambers (CoverWell PCI-0.5) and incubated at room temperature.

### Rheological test

The Oscillatory rheological results were collected from a AR G2 TA rheometer equipped with a parallel-plate made of stainless steel (diameter is 40 mm) and a solvent trap to prevent the evaporation of solvent from the samples. All the measurements were performed in a strain controlled mode at 25 $^{o}$C. The strain and the frequency for the time sweep measurements were set to 0.05% and 1.0 Hz, respectively. All the samples were prepared in 0.1 M phosphate buffer at pH 7.0. After mixing the stock solutions of the building blocks to the target concentration, the sample solution was transferred immediately onto the rheometer plate for the measurement.

### Determination of the gel composition

The composition of the tris-hydrazone products in the gel was analyzed by high performance liquid chromatography (HPLC) using a gradient eluent flow of $H_2O$:(MeOH+0.4% triethylamine (TEA)) linearly varied from a ratio of 8:2 to 2:8, referring to a previous study.[1] The samples for the HPLC measurements were prepared by adding 80 μL gel sample into a mixture solution of 400 μL THF and 400 μL TEA saturated $H_2O$. The ratio of various HGs was calculated using the UV absorbance at the isosbestic point (275 nm). HPLC-MS (Figure S3): **A**, elution time = 9.0 min, MS (ESI, positive) m/z = 365.4 $(M+Na)^{+}$; **A**$^{-}$, elution time = 1.45 min, MS (ESI, negative) m/z = 243.0 $(M-H)^{-}$; $\mathbf{HA_3}$, elution time = 15.3 min, MS (ESI, positive) m/z = 1253.55 $(M+Na)^{+}$; $\mathbf{HA_2A^-}$, elution time = 10.5 min, MS (ESI, negative) m/z = 584.3 $(M+2H_2O-2H)^{2-}$; $\mathbf{HAA^-_2}$, elution time = 2.4 min, MS (ESI, negative) m/z = 517.3 $(M-2H)^{2-}$, 534.0 $(M+2H_2O-2H)^{2-}$; $\mathbf{HA^-_3}$, elution time = 1.2 min, MS (ESI, negative) m/z = 317.0 $(M+H_2O-3H)^{3-}$.

**Cryo-TEM measurements**

A Gatan model 626 cryo-stage in a JEOL JEM 1400 Plus electron microscope was employed to characterize the morphologies of the gel networks. The operating voltage was 120 kV. For the measurements, 5 μL of the gel samples were carefully deposited on a Quantifoil R 1.2/1.3 100 Holey carbon films coated Cu 200 mesh grid. After blotting, the grid was rapidly inserted into liquid ethane. The frozen-hydrated sample was always stored in liquid nitrogen before the observation. The cryo-TEM images were recorded under low-dose conditions on a slow scan CCD camera (Gatan, model 830).

**Polarizing light microscope measurements**

A gelator precursor solution including 20 mM H, 120 mM (**A** + $\mathbf{A}^-$) (containing 30 mol% $\mathbf{A}^-$) in 0.1 M phosphate buffer at pH 7.0 was prepared and transferred into a glass chamber made by two glass slides with a PDMS spacer in between. After the gel formation, the network structures of the generated gel were analyzed on a Nikon E400POL polarizing microscope.

**Analysis of critical assembly concentration (CAC) of NGs and CGs**

For the **NGs** the critical gelation concentration (CGC) is known from previous work of our group and amounts to ~2 mM.[1,2,4] Because the CAC is always smaller than the CGC, we can confidently take this value of 2 mM as the upper limit of the CAC for the **NGs**: $CAC_{\mathbf{NG}} < 2$ mM. For the **CGs**, we have observed that gelation does not longer occur at a total gelator concentration of 20 mM if more than 40 mol% of $\mathbf{A}^-$ is present. The CLSM investigations, shown in Figure S13, revealed that even 24 h after preparation of the samples with addition of more than 40 mol% $\mathbf{A}^-$, still no fibers are formed. This is further confirmed by rheological measurement (Figure S14). Because at these conditions the samples contained > 0.7 **CGs** (14 mM) has stopped to self-assemble due to the electrostatic repulsion, we can confidently take the total gelator concentration of 20 mM used in these experiments as the lower limit for the CAC of the **CGs**: $CAC_{\mathbf{CG}} > 20$mM. Altogether, it is clear that the CAC of the **CGs** is at least 10 times higher than **NGs**. This large difference in CACs makes **NGs** reach their CAC prior to **CGs**, leading to earlier formation of **NFs** than **CFs**.

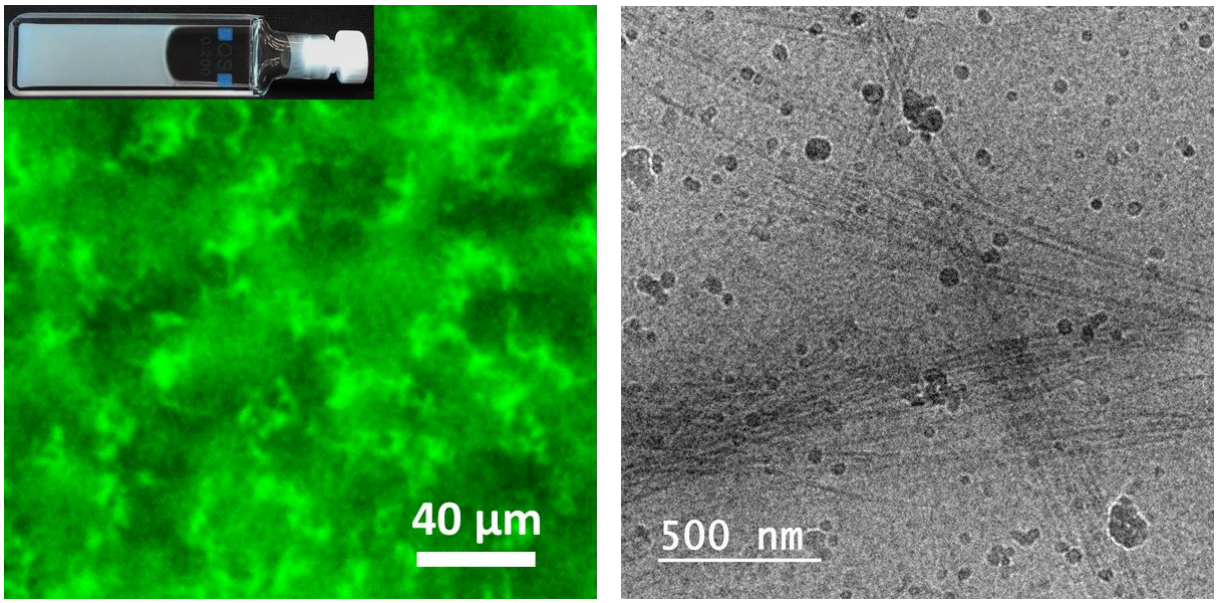


**Figure S1.** CLSM (left), and cryo-TEM (right) images of the gel prepared with 20 mM **H** and 120 mM **A** in 0.1 M phosphate buffer at pH 7.0, 30 µM **A-FL** was added to label the gel. Inset on the CLSM image is the photograph of the gel sample. The black balls on the cryo-TEM image are ice crystals which are formed during the preparation of cryo-TEM samples and are hard to avoid completely.[5]

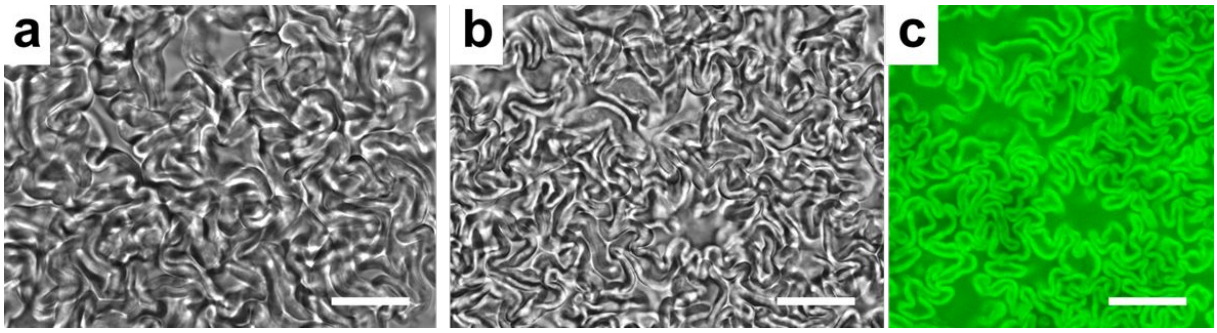


**Figure S2.** Bright field microscopy images of a) gel prepared without addition of probe **A-FL**; b) gel prepared with addition of 30 µM **A-FL**; and c) CLSM image corresponding to b). All the samples: [**H**] = 20 mM, [**A**] + [$\mathbf{A}^-$] = 120 mM (including 30 mol% $\mathbf{A}^-$). Scale bars = 40 µm.

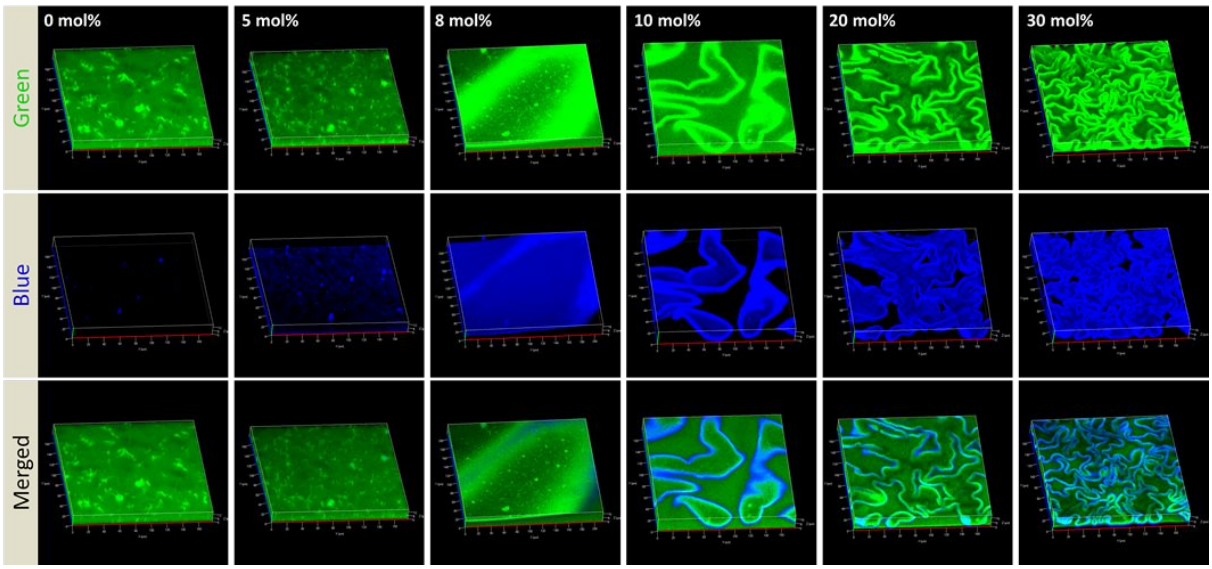


**Figure S3.** 3D CLSM images of the crumpled gel networks in different channels. Samples: [**H**] = 20 mM, [**A**] + [**A**$^-$] = 120 mM (including different mol% **A**$^-$), [**A-FL**] = 30 μM (green channel), [**Hoechst 33342**] = 20 μM (blue channel).

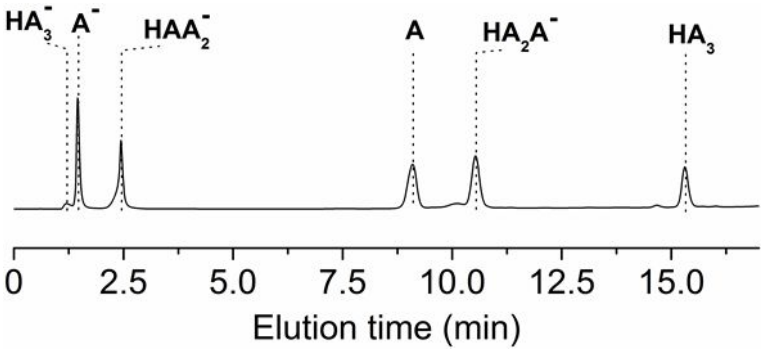


**Figure S4.** HPLC spectrum of the gel samples. The gel sample is prepared with 20 mM **H**, and 120 mM (**A** + **A**$^-$) (including 35 mol% **A**$^-$).

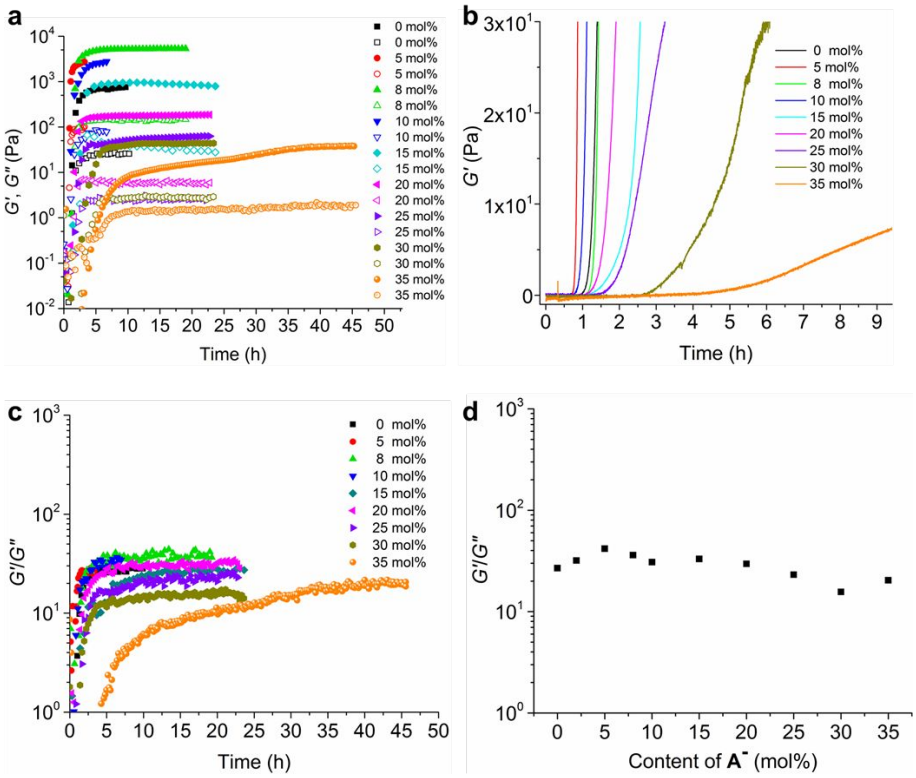


**Figure S5.** a) Evolution of *G'* (solid) and *G''* (hollow) against time for the samples prepared with different content of $\mathbf{A}^-$, b) magnified graph in a); c) *G'*/*G''* as a function of time; and d) plateau *G'*/*G''* as a function of the content of $\mathbf{A}^-$. Samples: [**H**] = 20 mM [**A**] + [$\mathbf{A}^-$] = 120 mM (containing different mol% $\mathbf{A}^-$).

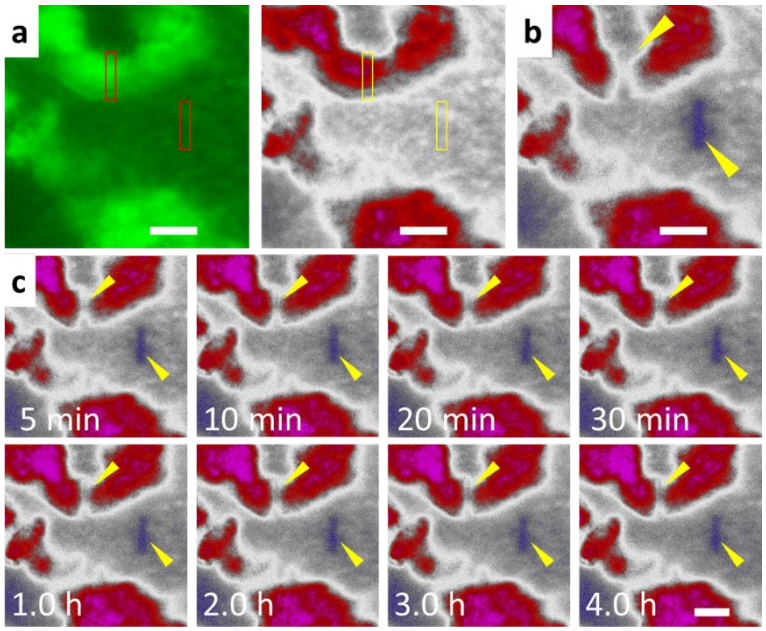


**Figure S6.** FRAP experiments of the gel networks a) before (rectangle areas), and b) after (yellow arrows) bleaching; c) evolution of the bleached areas over time. Sample: [**H**] = 20 mM, [**A**] + [$\mathbf{A}^-$] = 120 mM (30 mol% $\mathbf{A}^-$), [**A-FL**] = 30 μM. Scale bars = 10 μm. The fluorescence intensity of the bleached regions in both the crumpled sheets and the fibrous networks did not recover over a period of 4.0 h, indicating the crosslinked nature in both areas.

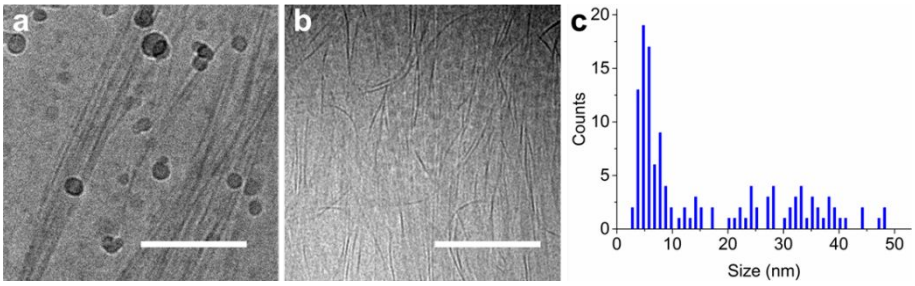


**Figure S7.** Cryo-TEM images of the gel fibers in the gel, a) area with more fibrous bundles; b) area with more thin fibers; and c) statistical size distribution of the fibers (bundles) in the gel sample, 130 fibers or bundles were randomly counted. Scale bars in a, b) are 200 nm. Sample: [**H**] = 20 mM, [**A**] + [**A**$^-$] = 120 mM (including 30 mol% **A**$^-$). The statistics of the dimensions of the fibers (bundles) were measured using Image J software. The black spheres on the cryo-TEM image are ice crystals formed during the preparation of cryo-TEM samples, which is very hard to avoid completely.[5]

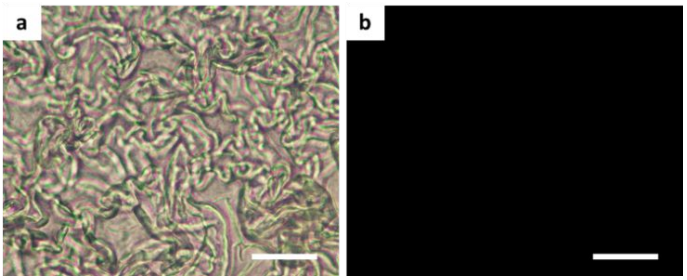


**Figure S8.** Polarizing light microscope images of the crumpled gel networks placed between a) parallel polarizer and b) crossed polarizers. Scale bars = 40 μm. Sample: [**H**] = 20 mM, [**A**] + [**A**$^-$] = 120 mM (including 30 mol% **A**$^-$).

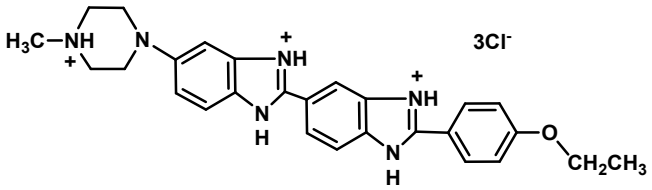


**Figure S9.** Chemical structure of **Hoechst 33342**.

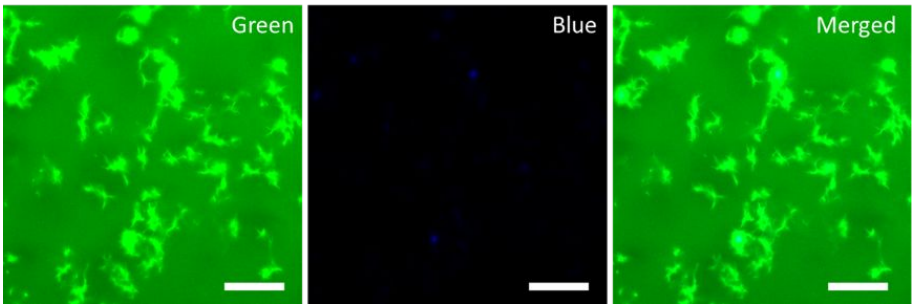


**Figure S10.** Confocal images of the gel networks prepared with pure **A**. Sample: [**H**] = 20 mM, [**A**] = 120 mM, [**A-FL**] = 30 μM (green), [**Hoechst 33342**] = 20 μM (blue). Scale bars = 40 μm. The ignorable fluorescent of **Hoechst**

**33342** in the blue channel indicates that there are no affinities between **Hoechst 33342** and **NFs**.

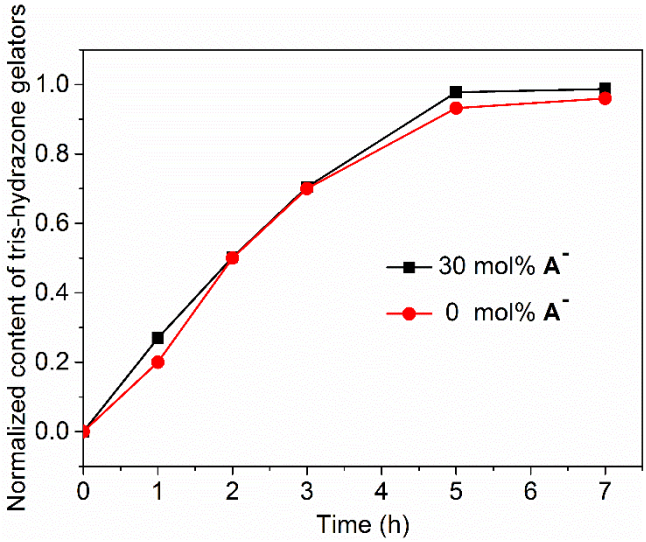


**Figure S11.** Formation of tris-hydrazone gelators over time monitored by HPLC. Samples: [**H**] = 20 mM, [**A**] + [**A**$^-$] = 120 mM (including 0 and 30 mol% **A**$^-$, respectively).

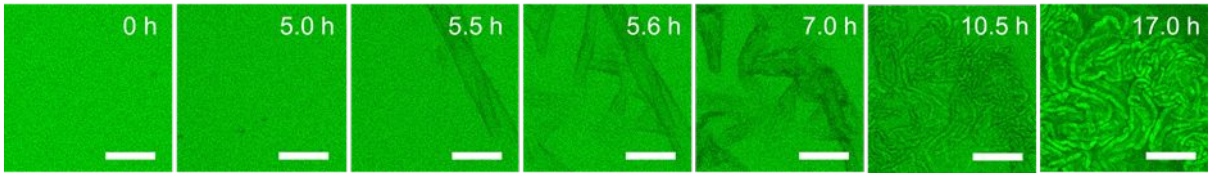


**Figure S12.** Formation of the gel networks without addition of **Hoechst 33342** over time, scale bars = 40 μm. Sample: [**H**] = 20 mM, [**A**] + [**A**$^-$] = 120 mM (30 mol% **A**$^-$), and [A-FL] = 30 μM.

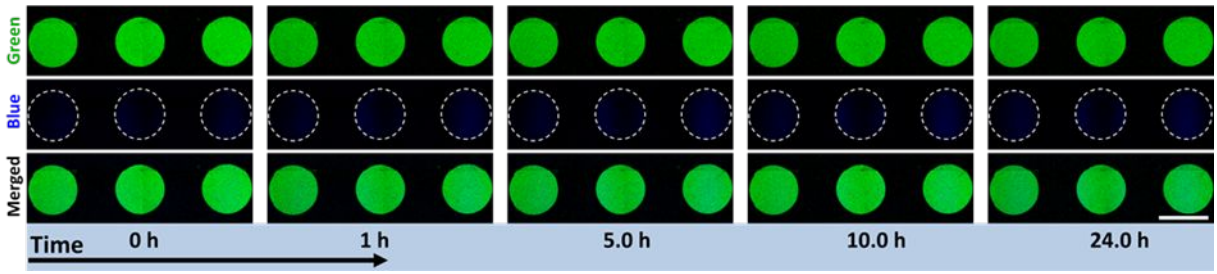


**Figure S13.** Fluorescence evolution in different channels over time. Sample: [**H**] = 20 mM [**A**] + [**A**$^-$] = 120 Mm (for each time point, the left sample 40 mol% **A**$^-$, the middle 45 and the right sample 50 mol%), [**A-FL**] = 30 μM (green channel), [**Hoechst 33342**] = 20 μM (blue channel). Scale bar for each subimage is 5 mm. The sample is prepared in a μ-Slide Angiogenesis (Ibidi) microscopy chamber with a glass bottom and sealed with grease. The ignorable fluorescence of **Hoechst 33342** in the blue channel demonstrates that very few **CFs** are formed in these samples though with high concentration of **CGs**, which we attribute to the electrostatic repulsions between the **CGs**. Apparently, the **CGs** cannot self-assemble independently at the concentrations used in the present work, which indicates the high CAC of **CGs**. These results strongly suggest that the **CFs** observed in this work are hybrid fibers

that are formed through co-assembly of **CGs** and **NGs**. In such hybrid fibers, the electrostatic repulsions between **CGs** would be released with the insertion of **NGs** in between.

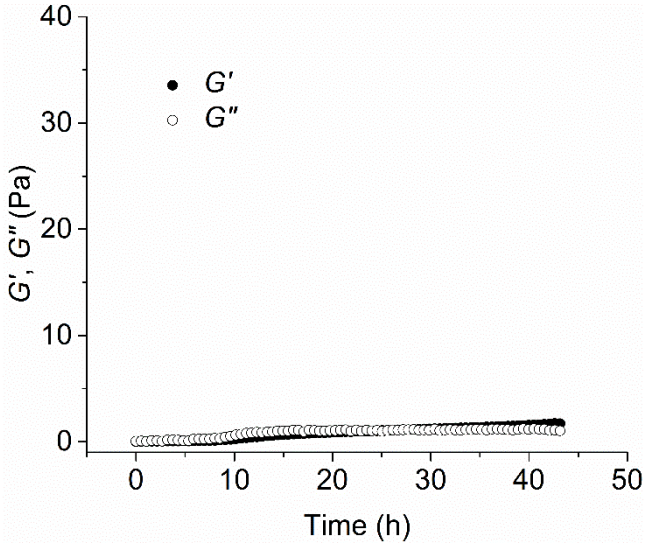


**Figure S14.** Evolution of *G'* and *G"* against time for the samples prepared with 45 mol% $\mathbf{A}^-$. Samples: [**H**] = 20 mM [**A**] + [$\mathbf{A}^-$] = 120 mM (45 mol% $\mathbf{A}^-$). The low *G'* with comparable value to *G"* indicates the absent formation of fibers in the solution though containing high concentration of **CGs**, which further demonstrates the high CAC of CGs.

## Reference


1. Boekhoven, J.; Poolman, J. M.; Maity, C.; Li, F.; van der Mee, L.; Minkenberg, C. B.; Mendes, E.; van Esch, J. H.; Eelkema, R., Catalytic control over supramolecular gel formation. *Nat. Chem.* **2013**, *5* (5), 433-7.
2. Poolman, J. M.; Boekhoven, J.; Besselink, A.; Olive, A. G.; van Esch, J. H.; Eelkema, R., Variable gelation time and stiffness of low-molecular-weight hydrogels through catalytic control over self-assembly. *Nat. Protoc.* **2014**, *9* (4), 977-88.
3. Suzuka, T.; Kimura, K.; Nagamine, T., Reusable Polymer-Supported Terpyridine Palladium Complex for Suzuki-Miyaura, Mizoroki-Heck, Sonogashira, and Tsuji-Trost Reaction in Water. *Polymers* **2011**, *3* (1), 621-639.
4. Wang, Y.; Versluis, F.; Oldenhof, S.; Lakshminarayanan, V.; Zhang, K.; Wang, Y.; Wang, J.; Eelkema, R.; Guo, X.; van Esch, J. H. *Adv. Mater.* **2018**, *30*, 1707408.
5. Franken, L. E.; Boekema, E. J.; Stuart, M. C. A., Transmission Electron Microscopy as a Tool for the Characterization of Soft Materials: Application and Interpretation. *Adv. Sci.* **2017,** *4* (5), 1600476.